



Published in final edited form as:

*J Biomed Mater Res A*. 2018 April ; 106(4): 971–984. doi:10.1002/jbm.a.36293.

## A Polyelectrolyte Multilayer Platform for Investigating Growth Factor Delivery Modes in Human Liver Cultures

Christine Lin<sup>a,b</sup>, Raimundo Romero<sup>a</sup>, Lioudmila V. Sorokina<sup>b</sup>, Kimberly R. Ballinger<sup>c</sup>, Laura W. Place<sup>a,d</sup>, Matt J. Kipper<sup>a,e</sup>, and Salman R. Khetani<sup>a,b,c</sup>

<sup>a</sup>School of Biomedical Engineering, Colorado State University, Fort Collins, CO

<sup>b</sup>Department of Bioengineering, University of Illinois at Chicago, Chicago, IL

<sup>c</sup>Department of Mechanical Engineering, Colorado State University, Fort Collins, CO

<sup>d</sup>Current address: Department of Biomedical Engineering, Tufts University, Medford, MA

<sup>e</sup>Department of Chemical and Biological Engineering, Colorado State University, Fort Collins, CO

### Abstract

Polyelectrolyte multilayers (PEMs) of chitosan and heparin are useful for mimicking growth factor (GF) binding to extracellular matrix (ECM) as *in vivo*. Here, we developed a PEM platform for delivering bound/adsorbed GFs to monocultures of primary human hepatocytes (PHHs) and PHH/non-parenchymal cell (NPC) co-cultures, which are useful for drug development and regenerative medicine. The effects of ECM protein coating (collagen I, fibronectin, and Matrigel®) and terminal PEM layer on PHH attachment/functions were determined. Then, heparin-terminated/fibronectin-coated PEMs were used to deliver varying concentrations of an adsorbed model GF, transforming growth factor  $\beta$  (TGF $\beta$ ), to PHH monocultures while using soluble TGF $\beta$  delivery via culture medium as the conventional control. Soluble TGF $\beta$  delivery caused a severe, monotonic, and sustained downregulation of all PHH functions measured (albumin and urea secretions, cytochrome-P450 2A6 and 3A4 enzyme activities), whereas adsorbed TGF $\beta$  delivery caused transient upregulation of 3 out of 4 functions. Finally, functionally stable co-cultures of PHHs and 3T3-J2 murine embryonic fibroblasts were created on the heparin-terminated/fibronectin-coated PEMs modified with adsorbed TGF $\beta$  to elucidate similarities and differences in functional response relative to the monocultures. In conclusion, chitosan-heparin PEMs constitute a robust platform for investigating the effects of GF delivery modes on PHH monocultures and PHH/NPC co-cultures.

### Keywords

transforming growth factor- $\beta$ ; fibroblasts; co-cultures; hepatocytes

## INTRODUCTION

*In vivo*, many growth factors (GFs) are bound to the glycosaminoglycan (GAG) side chains on proteoglycans in the extracellular matrix (ECM) and such binding can be regulated in a spatiotemporal manner by cell-secreted enzymes towards modulating cell functions.<sup>1</sup> In contrast, GFs are typically delivered to cells in soluble form via culture medium exchanges *in vitro*; however, such a protocol requires high concentrations of costly GFs to elicit a cellular response and frequent dosing due to the very short half-lives of GFs in an aqueous milieu. Furthermore, delivering GFs through culture medium may have non-physiologic effects on the cells as it does not mimic *in vivo*-like regulated presentation of bound GFs from the ECM.<sup>2,3</sup> On the other hand, polyelectrolyte multilayers (PEMs) containing ionically crosslinked layers of chitosan and heparin can be used to mimic GF binding to heparin and thus provide cells with a more *in vivo*-like signaling microenvironment.<sup>4</sup> Such chitosan-heparin PEMs have been successfully used to present heparin-bound fibroblast growth factor 2 (FGF-2) to bone marrow-derived ovine mesenchymal stem cells towards modulating their proliferation *in vitro*.<sup>5</sup>

Understanding how GFs affect isolated primary human hepatocytes (PHHs) in physiological and pathophysiological contexts is important for developing robust human liver platforms for applications such as drug toxicity screening, discovery of novel therapeutics, and regenerative medicine (i.e. cell-based therapies).<sup>6</sup> PHHs are a particularly attractive cell source for the above-mentioned applications because they are closer to human liver physiology than abnormal cancerous cell lines and animal hepatocytes, and are relatively straight-forward to use in medium- to high-throughput culture formats.<sup>7</sup> Compatibility of PEMs of various compositions with rat hepatocyte cultures has been shown, including poly(diallyldimethylammonium chloride)/sulfonated poly(styrene) (PDAC/SPS)<sup>8</sup>, poly(acrylic acid)/poly(allylamine hydrochloride)<sup>9</sup>, polyacrylic acid/polyethyleneimine<sup>10</sup>, and chitosan/DNA.<sup>11</sup> However, these studies did not culture PHHs on PEMs nor did they determine the effects of bound and soluble GFs on liver functions. Therefore, in this study, we developed a platform using chitosan/heparin PEMs that can be used for investigating GF signaling in short-term and long-term PHH cultures in an *in vivo*-like bound/adsorbed context. Protocols were first developed to enable optimal adhesion and functionality of PHHs on PEMs modified with ECM proteins (collagen I, fibronectin, and Matrigel®). Then, heparin-terminated PEMs coated with ECM protein were used to deliver a model GF, transforming growth factor  $\beta$  (TGF $\beta$ ), to PHH monocultures and the effects on diverse PHH functions were determined over several weeks relative to conventional delivery of soluble TGF $\beta$  via culture medium exchanges. Finally, functionally stable co-cultures of PHHs and 3T3-J2 murine embryonic fibroblasts were created on the heparin-terminated PEMs coated with ECM protein and the effects of adsorbed TGF $\beta$  delivery were determined on the co-culture phenotype and compared to results in monocultures.

## MATERIALS AND METHODS

### Preparation of polyelectrolyte multilayer (PEM) substrates

Chitosan was purchased from Novamatrix (Protasan UP B 90/20, 5% acetylated determined by <sup>1</sup>H NMR, MW = 80 kDa; PDI = 1.52; Sandvika, Norway) and heparin sodium was

purchased from Celsus Laboratories (from porcine intestinal mucosa, 12.5% sulfur, MW = 14.4 kDa; PDI = 1.14; Cincinnati, OH). Aqueous solutions were prepared at 0.01 M on a saccharide basis in acetate buffer (0.2 M, pH 5.0) and filtered through 0.22  $\mu\text{m}$  polyvinylidene fluoride syringe filters (Thermo Fisher Scientific, Waltham, MA) as previously described.<sup>5,12</sup> An acidified water rinse solution (acetic acid, pH 4.0) was also prepared and filtered. Layer-by-layer assembly of the polyelectrolyte solutions was employed by alternating 5-minute adsorption steps with 5-minute acidified water rinses in standard 24-well or 96-well tissue culture-treated polystyrene plates (TCPS, Corning Life Sciences, Tewksbury, MA). A 300- $\mu\text{L}$  or 50- $\mu\text{L}$  solution for 24-well and 96-well plates, respectively, was added to each well and adsorbed under gentle agitation. Due to TCPS being negatively charged, the first layer adsorbed to TCPS was always chitosan, which is positively charged. Heparin-terminated PEMs were constructed with six polyelectrolyte layers, whereas chitosan-terminated PEMs were constructed with seven layers for complete surface coverage. The PEMs-coated wells were washed three times with double-distilled water ( $\text{ddH}_2\text{O}$ ) prior to sterilization with 70% ethanol for 1 hour. The sterilized PEMs-coated wells were then washed three times with  $\text{ddH}_2\text{O}$  prior to TGF $\beta$  adsorption. Recombinant human TGF $\beta$ 1 (R&D Systems, Minneapolis, MN) was diluted to 100, 1000, and 10000 pg/mL, and allowed to adsorb in the PEM-coated wells for 2 hours under gentle agitation, followed by two  $\text{ddH}_2\text{O}$  rinses. ECM proteins including rat tail collagen I, fibronectin, or Matrigel (Corning Life Sciences) were adsorbed at concentrations ranging from 10–100  $\mu\text{g}/\text{mL}$  by exposing the wells to the protein solutions for 2 hours at 37°C, followed by two  $\text{ddH}_2\text{O}$  rinses. The plates were then stored at 4°C prior to cell seeding.

#### **Atomic force microscopy (AFM) and X-ray photoelectron spectroscopy (XPS) substrate surface characterization**

AFM was used to image the surface topographies of TCPS, heparin-terminated PEM-coated TCPS as well as PEMs-coated TCPS with TGF $\beta$  (300 pg/ml) only, fibronectin (100  $\mu\text{g}/\text{ml}$ ) only, or both TGF $\beta$  and fibronectin. TCPS and coated TCPS samples were cut out and adhered onto 50 mm glass-bottomed petri dishes for imaging. A Bruker BioScope Resolve BioAFM (Bruker AFM, Santa Barbara, CA) was used to obtain images. The microscope was located on a vibration isolation table (Technical Manufacturing Corporation, Peabody, MA) and housed within an acoustic enclosure (Herzan LLC, Laguna Hills, CA). All images were acquired using Bruker's Nanoscope software version 9.3 (Bruker AFM, Santa Barbara, CA) in the ScanAsyst® mode in air and at room temperature. A Bruker silicon nitride SNL probe was used and the cantilever used had a nominal spring constant of 0.35 N/m, resonance frequency of 65 kHz, and tip radius of 2 nm. An automated thermal tune was performed before each imaging session. The Peakforce setpoint, amplitude, and frequency were manually adjusted to obtain stable imaging conditions and to minimize noise. The typical line scan rate was 1–1.5 Hz. Square images (4  $\mu\text{m}$   $\times$  4  $\mu\text{m}$  and 800 nm  $\times$  800 nm) were acquired at a resolution of 256  $\times$  256 pixels. To obtain representative images, 2 samples of each treatment group were imaged with different areas imaged on each sample. Nanoscope Analysis version 1.8 (Bruker AFM, Santa Barbara, CA) was used for image analysis. AFM images were corrected with a plane fit before 3D images were made.

All sample surfaces were analyzed by XPS using a Physical Electronics 5800 spectrometer (Chanhasen, MN). Spectra were obtained using a monochromatic Al K $\alpha$  X-ray source ( $h\nu = 1486.6$  eV), a hemispherical analyzer, and multichannel detector. High-resolution spectra of O1s, N1s, C1s, and S2p envelopes were acquired at a pass energy of 23.5 eV, with 0.1 eV steps, a spot size of 800  $\mu\text{m}$ , and a takeoff angle of 45°. A low-energy electron gun was used for charge neutralization. Aliphatic carbon at 284.8 eV in the C1s envelope was used to align spectra. High-resolution spectra curve fits were performed using Phi Electronics Multipak version 9.3.0.3 (Chanhasen, MN).

### **Assessment of TGF $\beta$ adsorption and release on heparin-terminated PEMs via ELISA**

Triplicate wells of a 96-well TCPS plate were prepared with heparin-terminated PEMs, TGF $\beta$ , and fibronectin as mentioned previously. 100  $\mu\text{g}/\text{ml}$  of fibronectin and various concentrations of TGF $\beta$  (100, 1000, and 10000  $\text{pg}/\text{ml}$ ) were used. The TCPS microtiter plate was stored at 37°C during the experiment. TGF- $\beta$ 1 DuoSet ELISA (R&D Systems, Minneapolis, MN) was used to determine TGF $\beta$  adsorption to the PEMs following the manufacturer's instructions. Triplicate whole sample supernatants were immediately assayed and replenished with fresh PBS at D0 (0 hours), D0 (2 hours), D1, and D3. The amount of TGF $\beta$  adsorbed to samples was calculated via the difference between the adsorbed values and the observed ELISA values, and cumulative mass of TGF $\beta$  retained at each timepoint was calculated.

### **Cell culture**

Cryopreserved PHH vials (BioreclamationIVT, Baltimore, MD; Triangle Research Laboratories, Research Triangle Park, NC) were processed as previously described.<sup>13</sup> Cell viability was assessed using trypan blue exclusion and was found to be >80%. Liver-derived non-parenchymal cells were found to be < 1% of all the cells. Cells were resuspended in serum-free hepatocyte maintenance medium and seeded at 33,000 cells per well in a 96-well plate format or 200,000 cells per well in a 24-well plate format and left overnight for attachment. The culture supernatant was collected and replaced with fresh medium every other day for assessment of cell functionality (50  $\mu\text{L}/\text{well}$  for 96-well format and 300  $\mu\text{L}/\text{well}$  for 24-well format). For co-cultures, 3T3-J2 murine embryonic fibroblasts were resuspended in serum-containing hepatocyte maintenance medium and seeded ~24 hours post hepatocyte seeding (1 fibroblast:1 hepatocyte).

### **Quantification of hepatocyte adhesion and functionality**

Cell adhesion was assessed via double-stranded DNA (dsDNA) content in adherent cells. DNA concentration was measured using an AccuBlue dsDNA quantitation kit (Biotium, Hayward, CA) or a Quant-iT PicoGreen dsDNA assay kit (Molecular Probes, Eugene, OR). Culture supernatants were assayed for albumin levels using a competitive enzyme-linked immunosorbent assay (ELISA, MP Biomedicals, Santa Ana, CA) with horseradish peroxidase detection and 3,3',5,5'-tetramethylbenzidine (TMB, Rockland Immunochemicals, Boyertown, PA) as the substrate, as previously described.<sup>13</sup> Urea concentration in culture supernatants was assessed using a colorimetric endpoint assay utilizing diacetyl monoxime with acid and heat (Stanbio Labs, Boerne, TX).<sup>13</sup> CYP3A4 enzyme activity was measured by first incubating the cultures with substrate (luciferin-IPA

from Promega Life Sciences, Madison, WI) for 1 hour at 37°C and then detecting the luminescence of the produced metabolite (luciferin) according to the manufacturer's protocols. CYP2A6 enzyme activity was measured by incubating the cultures with coumarin for 1 hour at 37°C and measuring the fluorescent metabolite, 7-hydroxy-coumarin (Sigma-Aldrich, St. Louis, MO). Absorbance and luminescence for the aforementioned assays were measured using a BioTek (Winooski, VT) Synergy H1 multi-mode plate reader.

### Data analysis

Experiments were repeated 2+ times with 3+ wells per condition. Data from representative experiments are presented. Error bars on graphs represent standard deviations. Microsoft Excel and GraphPad Prism 7.0 (La Jolla, CA) were used for data analysis and graphing. Statistical significance was determined using the two-tailed Student's t-test assuming unequal variances or one-way ANOVA with *post-hoc* test (Tukey or Dunnett).

## RESULTS

### Effects of PEM terminal layer and ECM protein type on PHH attachment and functions

Chitosan and heparin PEMs were constructed on industry-standard TCPS plates. Figure 1A shows the chemical structures for both polyelectrolytes and Figure 1B depicts the process of preparing heparin-terminated PEMs modified with ECM protein and GF for cell culture. To create chitosan-terminated PEMs, 7 layers of polyelectrolytes were deposited instead of 6. Surface characterization demonstrated that our PEM construction process resulted in PEMs on the nanometer scale (Supplemental Figure 1). For nanometer-scale PEMs, biological responses have been shown to depend on the terminal layer.<sup>14</sup> Therefore, we sought to assess the effects of either a chitosan or heparin terminal layer on PHH attachment and functions on adsorbed ECM proteins (100 µg/mL in solution). The ECM proteins selected were rat tail collagen type I, human fibronectin, and Matrigel, which have been previously used for hepatocyte culture.<sup>7,13</sup> PHHs were cultured on these surfaces for up to 9 days and culture medium was collected every 2 days for quantification of liver functions that included albumin secretion (a surrogate for protein synthesis) and urea synthesis (a marker of nitrogen metabolism). Finally, at the end of the culture period (day 9), cells were lysed for dsDNA quantification as a measure of the differences in retention of adherent PHHs on the various surfaces. Since hepatocytes do not proliferate *in vitro* in the absence of GFs such as hepatocyte growth factor and epidermal growth factor<sup>15</sup>, dsDNA can serve as a measure of differences in the number of adherent cells.

We observed via phase contrast imaging that more PHHs attached to heparin-terminated PEMs coated with collagen (rat tail type I) as compared to chitosan-terminated PEMs (Figure 2A). The images also revealed that more cells attached to PEMs coated with fibronectin or Matrigel as compared to collagen. Quantification of dsDNA confirmed the phase contrast observations in that ~3.6-fold more dsDNA was measured on heparin-terminated PEMs versus chitosan-terminated PEMs coated with collagen (Figure 2B left). In contrast to collagen, the terminal layer did not significantly affect PHH retention when either fibronectin or Matrigel was used as the ECM coating. Across the various ECM coatings, chitosan-terminated PEMs modified with collagen had ~21% and ~22% of the dsDNA on

chitosan-terminated PEMs modified with fibronectin or Matrigel, respectively. Heparin-terminated PEMs modified with collagen had ~64% and ~72% of the dsDNA on heparin-terminated PEMs modified with fibronectin or Matrigel, respectively. Most of the aforementioned dsDNA trends were also observed with PHH albumin secretion (Figure 2B middle) and urea synthesis (Figure 2B right), except heparin-terminated PEMs coated with fibronectin led to ~ 2.2-fold higher albumin secretion from PHHs relative to the secretion from chitosan-terminated PEMs coated with fibronectin.

For all subsequent studies described below, we selected heparin-terminated PEMs coated with fibronectin since such a configuration a) allows for high levels of PHH attachment/retention and functions as compared to collagen, b) can be used to present heparin-bound GFs to the cells, and c) is not confounded by the many components present in a complex ECM like Matrigel that may interact differentially and in an unknown way with GFs with each lot/batch. The fibronectin concentration to coat heparin-terminated PEMs for all subsequent studies was chosen to be 100  $\mu\text{g}/\text{mL}$  since it led to highest hepatocyte attachment and functions as compared to lower fibronectin concentrations (Supplemental Figure 2).

### Surface characterization of substrates via AFM and XPS

Surface morphology characterization of heparin-terminated PEMs coated with fibronectin was performed with AFM. Representative AFM images and average root mean square roughness (Rq) values are shown in Figure 3 with scan sizes of  $4\ \mu\text{m} \times 4\ \mu\text{m}$  (top row) and  $800\ \text{nm} \times 800\ \text{nm}$  (bottom row). Neat TCPS images are seen in Figures 3A and 3F. Subsequent surface modification with heparin-terminated PEMs are in Figures 3B and 3G. Proteins, TGF $\beta$  and fibronectin, adsorbed separately or combined, are seen in Figures 3C–3E and 3H–3J. Generally, surfaces coated with either TGF $\beta$  or fibronectin separately or combined showed increased roughness and surface features compared to heparin-terminated PEM surfaces and neat TCPS, as also confirmed via increased average Rq values of modified TCPS.

XPS was used to characterize surface chemistry. Since XPS is a surface sensitive technique, it is capable of discerning differences in surface chemistry due to protein adsorption. The atomic percent compositions of the TCPS, chitosan-heparin PEMs, TGF $\beta$ -modified PEMs, fibronectin-modified PEMs, and fibronectin- and TGF $\beta$ -modified PEMs are shown in Table 1. As expected, TCPS only has detectable carbon and oxygen. Upon PEM addition, the carbon-to-oxygen ratio is reduced, and the nitrogen and sulfur content both increase, in line with the chemical structures of chitosan and heparin. Subsequent addition of TGF $\beta$  and fibronectin resulted in the reduction of detectable sulfur compared to PEM-modified TCPS. An increased nitrogen to sulfur ratio was observed in all protein-coated surfaces compared to protein-free surfaces, which further supports TGF $\beta$  and fibronectin adsorption on heparin-terminated PEMs. High resolution XPS spectra of the O1s, N1s, C1s, and S2p envelopes are shown in Figure 4.

### TGF $\beta$ retention on heparin-terminated PEMs with and without fibronectin

TGF $\beta$  adsorbed onto heparin-terminated PEMs with and without fibronectin was assessed using ELISA. Amounts of TGF $\beta$  adsorbed on samples as well as TGF $\beta$  cumulative retention

over 3 days are seen in Table 2. During sample preparation, TGF $\beta$  was always adsorbed before fibronectin, which resulted in samples with and without fibronectin adsorbing similar amounts of TGF $\beta$  for all TGF $\beta$  concentrations tested. Increased TGF $\beta$  solution concentrations resulted in increased amounts of TGF $\beta$  adsorption. Overall, we found that >70% of the TGF $\beta$  was adsorbed and subsequently retained over several days on the heparin-terminated PEMs, although fibronectin-coated samples retained less TGF $\beta$  compared to fibronectin-free samples.

### Modulation of PHH functions by TGF $\beta$ adsorbed to heparin-terminated PEMs

PHHs were seeded onto heparin-terminated PEMs with or without fibronectin coating, while PEMs-free TCPS coated with fibronectin served as the control substrate. A fibronectin coating on PEMs led to significantly higher PHH attachment relative to fibronectin-free PEMs as assessed by dsDNA levels of adherent cells 1 day after seeding (~4 fold more dsDNA). Furthermore, there were no significant differences in PHH attachment, morphology, albumin secretion, or urea synthesis on PEMs and TCPS coated with fibronectin (Figures 5A–D). Some minor differences were observed in CYP3A4 and CYP2A6 enzyme activities of PHHs across the two substrates (Figures 5E–F). Nonetheless, both PEMs and TCPS coated with fibronectin supported PHH functions for 3+ weeks, albeit functions were declining after ~1 week as expected from previous literature on PHH monocultures.<sup>13</sup>

On heparin-terminated PEM substrates coated with both TGF $\beta$  and fibronectin (no further TGF $\beta$  was added to the culture medium after the initial adsorption to PEMs), PHH albumin secretion over 21 days was similar at 100 pg/mL TGF $\beta$  to secretion from cultures on TGF $\beta$ -free PEMs (Figure 6A left). In contrast, 1000 and 10000 pg/mL of adsorbed TGF $\beta$  caused a downregulation of albumin secretion to ~51–66% of secretion from cultures on TGF $\beta$ -free PEMs after 7 days; however, such drastic effects were not observed after 15 and 21 days of culture. Urea synthesis from PHH cultures treated with 100 pg/mL and 1000 pg/mL TGF $\beta$  was transiently increased in a dose-dependent manner relative to TGF $\beta$ -free PEMs (i.e. 1.1 fold and 1.3 fold with 100 pg/mL and 1000 pg/mL TGF $\beta$ , respectively, after 15 days in culture) (Figure 6B left).

CYP3A4 activity in PHH cultures increased transiently ~1.4-fold after 7 days on 100 and 1000 pg/mL of adsorbed TGF $\beta$  relative to TGF $\beta$ -free PEMs, but showed some decrease (~21–34%) after 13 and 21 days in culture at the same TGF $\beta$  doses (Figure 6C left). Finally, CYP2A6 activity in PHH cultures increased transiently ~1.5–1.6-fold after 7 days on 100 pg/mL and 1000 pg/mL of adsorbed TGF $\beta$ , while after 21 days, cultures on 1000 pg/mL and 10000 pg/mL of adsorbed TGF $\beta$  had higher CYP2A6 activity than activity in cultures on TGF $\beta$ -free PEMs (Figure 6D left).

### Modulation of PHH functions by soluble TGF $\beta$ in culture medium

For comparison with PHH functions on TGF $\beta$ -modified PEMs, we also created PHH cultures on fibronectin-coated TCPS and dosed cultures with soluble TGF $\beta$  in culture medium (conventional methodology). One set of such cultures was treated with TGF $\beta$  once over 2 days (1 soluble TGF $\beta$ ), while another set of cultures was treated repeatedly with fresh

TGF $\beta$  every 2 days over several weeks (continuous). Both the single treatment (Figure 6A middle) and continuous treatment (Figure 6A right) with soluble TGF $\beta$  led to downregulation of albumin secretion from cultures across all timepoints and all TGF $\beta$  concentrations, albeit quantitative differences were observed across the two soluble delivery profiles after 15 and 21 days in culture. Specifically, after 15 days, continuous treatment with soluble TGF $\beta$  at 100 pg/mL, 1000 pg/mL, and 10000 pg/mL downregulated albumin secretion from cultures to ~23%, ~1%, and ~4% of secretion from cultures on the TGF $\beta$ -free TCPS, respectively; in contrast, a single treatment with soluble TGF $\beta$  at 100 pg/mL, 1000 pg/mL, and 10000 pg/mL downregulated albumin secretion to ~56%, 37%, and ~2%, respectively. After 21 days, continuous treatment with soluble TGF $\beta$  at 100 pg/mL, 1000 pg/mL, and 10000 pg/mL downregulated albumin secretion to ~24%, ~5%, and ~15% of secretion from cultures on the TGF $\beta$ -free TCPS, respectively, whereas a single treatment with soluble TGF $\beta$  at 100 pg/mL, 1000 pg/mL, and 10000 pg/mL downregulated albumin secretion from cultures to ~56%, ~45%, and ~55%, respectively.

Urea synthesis showed similar trends as albumin for PHH cultures treated a single time (Figure 6B middle) or continuously (Figure 6B right) with soluble TGF $\beta$ . After 15 days, continuous treatment with soluble TGF $\beta$  at 100 pg/mL, 1000 pg/mL, and 10000 pg/mL downregulated urea synthesis in cultures to ~42%, ~14%, and ~18% of the synthesis in cultures on TGF $\beta$ -free TCPS, respectively; in contrast, a single treatment with soluble TGF $\beta$  at 100 pg/mL, 1000 pg/mL, and 10000 pg/mL downregulated urea synthesis in cultures to ~72%, 63%, and ~15%, respectively. After 21 days, continuous treatment with soluble TGF $\beta$  at 100 pg/mL, 1000 pg/mL, and 10000 pg/mL downregulated urea synthesis in cultures to ~26%, ~8%, and ~11% of synthesis in cultures on TGF $\beta$ -free TCPS, respectively, whereas a single treatment with soluble TGF $\beta$  at 100 pg/mL, 1000 pg/mL, and 10000 pg/mL downregulated urea synthesis in cultures to ~60%, ~36%, and ~13%, respectively.

As with albumin and urea secretions, CYP450 enzyme activities displayed a more severe downregulation in cultures treated continuously with soluble TGF $\beta$  as compared to cultures treated a single time with soluble TGF $\beta$ . After 13 days, continuous treatment with soluble TGF $\beta$  (Figure 6C right) at 100 pg/mL, 1000 pg/mL, and 10000 pg/mL downregulated CYP3A4 activity in cultures to ~28%, <1%, and <1% of the activity in cultures on TGF $\beta$ -free TCPS, respectively; in contrast, a single treatment with soluble TGF $\beta$  (Figure 6C middle) at 100 pg/mL, 1000 pg/mL, and 10000 pg/mL downregulated CYP3A4 activity in cultures to ~67%, 51%, and <1%, respectively. After 21 days, continuous treatment with soluble TGF $\beta$  at 100 pg/mL, 1000 pg/mL, and 10000 pg/mL downregulated CYP3A4 activity in cultures to ~5%, ~1%, and ~2% of activity in cultures on TGF $\beta$ -free TCPS, respectively, whereas a single treatment with soluble TGF $\beta$  at 100 pg/mL and 1000 pg/mL upregulated activity in cultures to ~1.3 fold and ~1.7 fold, respectively. At 10000 pg/mL of soluble TGF $\beta$  under a single treatment, CYP3A4 activity in cultures displayed a downregulation to ~16% of activity in cultures on TGF $\beta$ -free TCPS. For CYP2A6, after 13 days, continuous treatment with soluble TGF $\beta$  (Figure 6D right) at 100 pg/mL, 1000 pg/mL, and 10000 pg/mL downregulated activity in cultures to ~41%, ~34%, and ~41% of the activity in cultures on TGF $\beta$ -free TCPS, respectively; in contrast, a single treatment with soluble TGF $\beta$  (Figure 6D middle) at 100 pg/mL, 1000 pg/mL, and 10000 pg/mL



downregulated CYP2A6 activity in cultures to ~84%, ~57%, and ~57%, respectively. After 21 days, CYP2A6 activity in all cultures was very low or undetectable.

### **Differences between modulation of PHH functions by adsorbed or soluble TGF $\beta$**

As discussed above, functions in PHH monocultures displayed significant differences across adsorbed or soluble delivery modes for TGF $\beta$ . Specifically, conventional delivery of soluble TGF $\beta$  via culture medium exchanges was more detrimental to diverse PHH functions (albumin, urea, CYP3A4/2A6 activities) over the course of 3 weeks than TGF $\beta$  adsorbed to heparin-coated PEMs, which instead caused transient upregulation of some functions (i.e. urea, CYP3A4, and CYP2A6) over the first week of culture relative to TGF $\beta$ -free control cultures. Such differences in PHH functions across the TGF $\beta$  presentation modes could be due to differential PHH death; however, phase contrast micrographs displayed similar adherent PHH density across conditions over time (Supplemental Figure 3), which suggests downregulation of PHH functions. Lastly, downregulation of PHH functions with soluble TGF $\beta$  treatment as compared to adsorbed TGF $\beta$  was also confirmed using a coating of 100  $\mu\text{g}/\text{mL}$  Matrigel (data not shown), which suggests that the results are not dependent on the ECM protein coating.

### **Creation of PHH-fibroblast co-cultures on heparin-terminated PEMs**

PHH monocultures discussed above, irrespective of substrate type or TGF $\beta$  delivery mode, displayed downregulation of all functions over 3 weeks, which is consistent with previous literature showing that neither ECM proteins nor specific soluble factors can fully stabilize the PHH phenotype.<sup>6</sup> In contrast, co-cultures of PHHs and 3T3-J2 murine embryonic fibroblasts on ECM protein-coated TCPS are known to display high levels of functions over several weeks as compared to pure PHH monocultures.<sup>13</sup> Therefore, here we first sought to determine the compatibility of heparin-terminated and fibronectin-coated PEMs for PHH-fibroblast co-cultures (1 PHH:1 fibroblast). We observed that both cell types were able to attach to and spread on heparin-terminated PEMs coated with 100  $\mu\text{g}/\text{mL}$  fibronectin (Figure 7A). However, in contrast to PHH monocultures, we found that supplementation of the culture medium with 10% bovine serum was required to maintain the co-cultures, likely due to the dependency of fibroblast spreading/growth on serum proteins. In serum-supplemented culture medium, PHHs in co-cultures maintained prototypical morphology (i.e. polygonal shape, distinct nuclei/nucleoli, and visible bile canaliculi) on fibronectin-coated PEMs and TCPS control surfaces for 3+ weeks.

Consistent with morphology, PHHs in co-cultures on fibronectin-coated PEMs and TCPS control surfaces displayed relatively stable functions for 3+ weeks, and such functions were significantly higher than those measured in PHH monocultures. Albumin secretion (Figure 7B) and urea synthesis (Figure 7C) from co-cultures on PEMs were similar to functions in co-cultures on TCPS; CYP3A4 activity (Figure 7D) in co-cultures on TCPS was higher than activity in co-cultures on PEMs across all timepoints (~1.4 fold on day 9 and 1.04 fold on days 16 and 23); and, CYP2A6 activity (Figure 7E) in co-cultures on TCPS was transiently higher (~1.3 fold on day 9) than activity in co-cultures on PEMs.

### Modulation of co-culture functions by TGF $\beta$ adsorbed to heparin-terminated PEMs

Next, we determined the effects of TGF $\beta$  adsorbed to heparin-terminated and fibronectin-coated PEMs on PHH functions in stable co-cultures using the same TGF $\beta$  concentrations as those used for PHH monocultures. Albumin secretion (Figure 8A) from co-cultures on PEMs was downregulated by adsorbed TGF $\beta$  at 100 pg/mL and 1000 pg/mL (but not at 10000 pg/mL) to ~84–98% of secretion from co-cultures on TGF $\beta$ -free PEMs. Similar to albumin secretion, adsorbed TGF $\beta$  caused downregulation of urea synthesis (Figure 8B) from co-cultures on PEMs as compared to co-cultures on TGF $\beta$ -free PEMs. After 15 days, adsorbed TGF $\beta$  at 100 pg/mL, 1000 pg/mL, and 10000 pg/mL all downregulated urea synthesis in co-cultures to ~82%, ~63%, and ~72%, of the synthesis in cultures on TGF $\beta$ -free PEMs, respectively, and such downregulation was similar at 21 days.

CYP3A4 activity (Figure 8C) in co-cultures on TGF $\beta$ -modified PEMs was downregulated to ~65–69% and ~88–90% by 7 and 13 days, respectively, at TGF $\beta$  concentrations up to 1000 pg/mL relative to activity in co-cultures on TGF $\beta$ -free PEMs. However, at 10000 pg/mL TGF $\beta$ , CYP3A4 activity was similar to activity in co-cultures on TGF $\beta$ -free PEMs after 7 and 13 days, and upregulated ~1.3 fold after 21 days. On the other hand, CYP2A6 activity (Figure 8D) in co-cultures was enhanced by adsorbed TGF $\beta$  over 3 weeks. For instance, after 21 days, CYP2A6 activity in co-cultures on PEMs was upregulated ~1.2–1.3 fold by adsorbed TGF $\beta$  at 1000 pg/mL and 10000 pg/mL.

## DISCUSSION

We developed a platform containing chitosan/heparin PEMs to investigate the long-term effects of heparin-bound GFs on PHH functions in monocultures and co-cultures with NPCs. The type of ECM protein coating and the terminal layer for the PEMs (chitosan vs. heparin) were shown to significantly affect PHH attachment and functions. Furthermore, PHH functions were found to be differentially sensitive to the mode of GF (TGF $\beta$  used as a model) delivery, either adsorbed to heparin-terminated PEMs or solubilized in culture medium for single or continuous treatment (conventional methodology). Finally, similarities and differences were observed in the functional response of co-cultures to adsorbed TGF $\beta$  delivery relative to the monocultures.

Fibronectin and Matrigel facilitated PHH attachment/functions on both chitosan- and heparin-terminated PEMs. Fibronectin is negatively-charged at physiological pH (isoelectric point of 5.2), which may facilitate binding to positively-charged chitosan via electrostatic interactions.<sup>16</sup> Additionally, heparin contains binding sites for fibronectin.<sup>17</sup> In contrast to purified fibronectin, Matrigel is an ECM mixture extracted from a mouse sarcoma containing laminin, entactin, collagen, and heparan sulfate proteoglycans.<sup>18</sup> Thus, PEMs can be modified with either purified ECM proteins or complex mixtures to enable cell attachment.

In contrast to fibronectin and Matrigel, rat tail type I collagen, which is widely used for hepatocyte culture<sup>6</sup>, facilitated better PHH attachment/functions on heparin-terminated PEMs than on chitosan-terminated PEMs. Heparin can bind to type I collagen independent of collagen's aggregation state<sup>19</sup>, and such binding occurs on the N-terminal basic triple

helical domain that is represented once within each collagen monomer and at multiple sites within collagen fibrils.<sup>20</sup> Lack of cell retention on chitosan-terminated PEMs coated with collagen suggests that collagen either did not properly adsorb to the chitosan layer and/or formed a non-uniform coating. Chitosan is a weak polycation with pendant amine groups that have  $pK_a \approx 6.4$ . At the neutral pH used for the protein adsorption, the free amine groups (not electrostatically bound to heparin in the PEM) are mostly deprotonated, making the surface considerably more hydrophobic, and possibly leading to non-uniform collagen adsorption. However, further molecular-scale studies would be required to determine the deposition and conformation of collagen on chitosan-terminated PEMs. Others have shown that covalently cross-linking collagen to chitosan layers can aid in cell attachment.<sup>21</sup> We did not execute such a strategy in this study since the effects of the crosslinker on PHH adhesion/functionality would first need to be characterized prior to incorporation into a PEM layer. Furthermore, since both fibronectin and Matrigel promoted sufficient PHH attachment/functions on heparin-terminated PEMs, which are suited for GF delivery, we proceeded with testing GF delivery to PHH cultures/co-cultures using fibronectin as the ECM protein of choice given the batch-to-batch variability inherent in a complex ECM mixture like Matrigel.

Heparin-terminated and fibronectin-coated PEMs adequately supported the attachment and functions of PHH monocultures as compared to the fibronectin-coated TCPS control used by others in the field. Some differences in CYP450 activities were observed over time across the substrate types; however, these differences were minor (<1.4 fold) and the cultures displayed similar kinetics of functions on both substrates. These results show that modification of TCPS with PEMs does not significantly affect PHH ability to attach and function for several weeks.

To demonstrate GF delivery from heparin-terminated PEMs to PHH cultures, we chose TGF $\beta$  since it plays a critical role in liver physiology/pathophysiology and has been shown to modulate hepatocyte functions *in vitro*.<sup>22</sup> *In vivo*, TGF $\beta$  binds to GAGs such as heparin and heparan sulfate for localized activity and prevention of degradation by enzymes.<sup>23</sup> *In vitro* studies have shown that when TGF $\beta$  is bound to heparin, its half-life is tripled, the amount of cell-associated TGF $\beta$  is doubled, and TGF $\beta$  activity is increased.<sup>24,25</sup> Chitosan is similar to other GAGs and can form ionic complexes with heparin.<sup>26</sup> We confirmed TGF $\beta$  adsorption to heparin-terminated PEMs via AFM and XPS. Additionally, the amounts of adsorbed (>70%) and released TGF $\beta$  over several days were assessed using ELISA on supernatants. In previous studies, we have shown FGF-2 delivery from chitosan/heparin PEMs<sup>5</sup> and thus, we anticipate that our platform can be used to deliver different GFs and mixtures to human liver cultures.

Delivery of soluble TGF $\beta$  to PHH monocultures on fibronectin-coated TCPS via culture medium exchanges (conventional methodology) caused a monotonic decline in diverse liver functions as a function of time and GF concentration. Surprisingly, even a single treatment with TGF $\beta$  over a 2-day medium exchange was generally detrimental to the cultures even after several weeks; continuous treatment with TGF $\beta$  with every medium exchange further accelerated the functional decline of the monocultures. On the other hand, adsorbed TGF $\beta$  did not lead to sustained downregulation of liver functions in PHH monocultures, and even

caused transient upregulation of 3 out of 4 functions over time. The differences in PHH functions due to TGF $\beta$  delivery modes are likely not due to differences in exposure of PHHs to varying amounts of TGF $\beta$  since we found that more than 70% of the TGF $\beta$  adsorbed to the heparin-terminated and fibronectin-coated PEMs and was retained over several days of measurement. Instead, we anticipate that as *in vivo*, PHHs respond differentially to adsorbed TGF $\beta$  as opposed to the solubilized form. Indeed, others have also demonstrated that the mode of GF presentation to cells can make a difference in terms of cell aggregation, spreading, and function.<sup>2,3</sup> Our platform now provides the avenue to study physiologically relevant PHH-GF interactions, while using significantly lower amounts of costly GFs than required for soluble delivery.

As expected from the previous studies<sup>6,13</sup>, ECM protein and GF alone were not sufficient to stabilize PHH phenotype in monocultures. In contrast, co-culture with both liver- and non-liver-derived NPC types has been long known to induce functions in primary hepatocytes from multiple species, including humans, which suggests that the molecular mediators underlying the 'co-culture effect' are relatively well-conserved across species.<sup>27,28</sup> Khetani and Bhatia have demonstrated that 3T3-J2 fibroblasts induce high levels of functions in PHHs<sup>13</sup>, which is likely due to the ability of the 3T3-J2 fibroblasts to express diverse hepatocyte-supportive molecules present in the liver, such as decorin<sup>29</sup> and T-cadherin.<sup>30</sup> Furthermore, the use of 3T3-J2 fibroblasts in co-culture with PHHs does not prevent the effective use of the stabilized PHHs for many applications in drug development (i.e. drug toxicity assessment, and hepatitis B/C viral infections).<sup>31-39</sup> Therefore, here we created co-cultures of PHHs and 3T3-J2 fibroblasts on heparin-terminated and fibronectin-coated PEMs and compared the long-term morphology and functions to those obtained on fibronectin-coated TCPS (conventional methodology). Overall, PEMs supported a stable PHH morphology and diverse functions for 3+ weeks at comparable levels as those observed in TCPS controls.

Delivering TGF $\beta$  to co-cultures at the same concentrations as those used for PHH monocultures revealed some key differences in functional responses between the two culture models. Specifically, adsorbed TGF $\beta$  at the higher doses, 1000 and 10000 pg/mL, downregulated albumin secretion in PHH monocultures after 7 days whereas no such downregulation was observed in co-cultures. Furthermore, while urea synthesis and CYP3A4 activity were transiently upregulated in PHH monocultures over 7 days due to 1000 pg/mL of adsorbed TGF $\beta$ , these functions in co-cultures were downregulated at the same timepoint; however, by 21 days, 10000 pg/mL of adsorbed TGF $\beta$  caused upregulation of CYP3A4 activity in both PHH monocultures and co-cultures. CYP2A6 activity was upregulated in both PHH monocultures and co-cultures over 3 weeks, albeit at different fold changes. The above-mentioned similarities and differences in functional responses of PHH monocultures and co-cultures to the same concentrations of adsorbed TGF $\beta$  on the same substrate could be due to several reasons. First, serum in the culture medium was required for obtaining high functions in co-cultures (due to optimal fibroblast growth and spreading), whereas PHH monocultures do not need serum to survive and serum can be detrimental to monocultures as shown previously.<sup>40</sup> It may be that serum proteins bind TGF $\beta$  and modulate its effects on PHHs in co-cultures relative to monocultures. Second, functionally stable PHHs in co-cultures may have a differential sensitivity to TGF $\beta$  than functionally declining

PHHs in monocultures. Finally, 3T3-J2s have been shown to express decorin<sup>29</sup>, a small leucine-rich proteoglycan that is known to bind to TGF $\beta$  and modulate its activity.<sup>41</sup> We plan to investigate these potential differences in TGF $\beta$  signaling across monocultures and co-cultures in future detailed studies.

In conclusion, PHH monocultures and PHH-fibroblast co-cultures were successfully established on chitosan-heparin PEMs coated with ECM proteins. Delivering the model GF, TGF $\beta$ , to the monocultures in adsorbed form via heparin-terminated PEMs yielded more complex concentration and time effects on PHH functions as compared to a monotonic and severe functional decline with soluble TGF $\beta$  delivery. Finally, functional response of co-cultures to adsorbed TGF $\beta$  showed similarities and differences across different liver functions to the response of monocultures. In the future, our platform can be extended to investigating the roles of diverse ECM proteins and GFs on human liver models of varying cellular compositions.

## Supplementary Material

Refer to Web version on PubMed Central for supplementary material.

## Acknowledgments

We thank Dustin Berger, Matthew Davidson, and Brenton Ware for their insightful discussions and assistance with cell culture. This work was supported by Colorado State University, NSF (CAREER award CBET-1351909 to S.R.K. and DBI-1531921 to M.J.K.), and NIH (1R03EB019184-01 to S.R.K.).

## References

1. Schönherr E, Hausser HJ. Extracellular matrix and cytokines: a functional unit. *Developmental immunology*. 2000; 7(2–4):89–101. [PubMed: 11097204]
2. Kuhl PR, Griffith-Cima LG. Tethered epidermal growth factor as a paradigm for growth factor-induced stimulation from the solid phase. *Nat Med*. 1996; 2(9):1022–7. [PubMed: 8782461]
3. Mehta G, Williams CM, Alvarez L, Lesniewski M, Kamm RD, Griffith LG. Synergistic effects of tethered growth factors and adhesion ligands on DNA synthesis and function of primary hepatocytes cultured on soft synthetic hydrogels. *Biomaterials*. 2010; 31(17):4657–71. [PubMed: 20304480]
4. Boddohi S, Killingsworth CE, Kipper MJ. Polyelectrolyte multilayer assembly as a function of pH and ionic strength using the polysaccharides chitosan and heparin. *Biomacromolecules*. 2008; 9(7):2021–2028. [PubMed: 18564872]
5. Almodóvar J, Bacon S, Gogolski J, Kisiday JD, Kipper MJ. Polysaccharide-based polyelectrolyte multilayer surface coatings can enhance mesenchymal stem cell response to adsorbed growth factors. *Biomacromolecules*. 2010; 11(10):2629–2639. [PubMed: 20795698]
6. Khetani SR, Berger DR, Ballinger KR, Davidson MD, Lin C, Ware BR. Microengineered liver tissues for drug testing. *Journal of laboratory automation*. 2015; 20(3):216–250. [PubMed: 25617027]
7. Godoy P, Hewitt NJ, Albrecht U, Andersen ME, Ansari N, Bhattacharya S, Bode JG, Bolleyn J, Borner C, Böttger J, et al. Recent advances in 2D and 3D in vitro systems using primary hepatocytes, alternative hepatocyte sources and non-parenchymal liver cells and their use in investigating mechanisms of hepatotoxicity, cell signaling and ADME. *Archives of toxicology*. 2013; 87(8):1315–1530. [PubMed: 23974980]
8. Kidambi S, Lee I, Chan C. Controlling primary hepatocyte adhesion and spreading on protein-free polyelectrolyte multilayer films. *Journal of the American Chemical Society*. 2004; 126(50):16286–16287. [PubMed: 15600306]

9. Chen AA, Khetani SR, Lee S, Bhatia SN, Van Vliet KJ. Modulation of hepatocyte phenotype in vitro via chemomechanical tuning of polyelectrolyte multilayers. *Biomaterials*. 2009; 30(6):1113–1120. [PubMed: 19046762]
10. Janorkar AV, Rajagopalan P, Yarmush ML, Megeed Z. The use of elastin-like polypeptide-polyelectrolyte complexes to control hepatocyte morphology and function in vitro. *Biomaterials*. 2008; 29(6):625–632. [PubMed: 18006054]
11. Rajagopalan P, Shen CJ, Berthiaume F, Tilles AW, Toner M, Yarmush ML. Polyelectrolyte Nanoscaffolds for the Design of Layered Cellular Architectures. *Tissue engineering*. 2006; 12(6):1553–1563. [PubMed: 16846351]
12. Almodóvar J, Place LW, Gogolski J, Erickson K, Kipper MJ. Layer-by-layer assembly of polysaccharide-based polyelectrolyte multilayers: a spectroscopic study of hydrophilicity, composition, and ion pairing. *Biomacromolecules*. 2011; 12(7):2755–2765. [PubMed: 21644518]
13. Khetani SR, Bhatia SN. Microscale culture of human liver cells for drug development. *Nature biotechnology*. 2008; 26(1):120–126.
14. Serizawa T, Yamaguchi M, Akashi M. Alternating bioactivity of polymeric layer-by-layer assemblies: anticoagulation vs procoagulation of human blood. *Biomacromolecules*. 2002; 3(4): 724–731. [PubMed: 12099816]
15. Bowen WC, Michalopoulos AW, Orr A, Ding MQ, Stolz DB, Michalopoulos GK. Development of a chemically defined medium and discovery of new mitogenic growth factors for mouse hepatocytes: mitogenic effects of FGF1/2 and PDGF. *PLoS ONE*. 2014; 9(4):e95487. [PubMed: 24743506]
16. Wittmer CR, Phelps JA, Saltzman WM, Van Tassel PR. Fibronectin terminated multilayer films: protein adsorption and cell attachment studies. *Biomaterials*. 2007; 28(5):851–860. [PubMed: 17056106]
17. Kan M, Shi EG. Fibronectin, not laminin, mediates heparin-dependent heparin-binding growth factor type I binding to substrata and stimulation of endothelial cell growth. *In vitro cellular & developmental biology: journal of the Tissue Culture Association*. 1990; 26(12):1151–1156. [PubMed: 1706698]
18. Hughes CS, Postovit LM, Lajoie GA. Matrigel: a complex protein mixture required for optimal growth of cell culture. *Proteomics*. 2010; 10(9):1886–90. [PubMed: 20162561]
19. San Antonio JD, Lander AD, Karnovsky MJ, Slayter HS. Mapping the heparin-binding sites on type I collagen monomers and fibrils. *The Journal of cell biology*. 1994; 125(5):1179–1188. [PubMed: 8195298]
20. Sweeney SM, Guy CA, Fields GB, San Antonio JD. Defining the domains of type I collagen involved in heparin-binding and endothelial tube formation. *Proceedings of the National Academy of Sciences of the United States of America*. 1998; 95(13):7275–7280. [PubMed: 9636139]
21. Wang XH, Li DP, Wang WJ, Feng QL, Cui FZ, Xu YX, Song XH, van der Werf M. Crosslinked collagen/chitosan matrix for artificial livers. *Biomaterials*. 2003; 24(19):3213–3220. [PubMed: 12763448]
22. Chia S-M, Lin P-C, Yu H. TGF-beta1 regulation in hepatocyte-NIH3T3 co-culture is important for the enhanced hepatocyte function in 3D microenvironment. *Biotechnology and bioengineering*. 2005; 89(5):565–573. [PubMed: 15669090]
23. Lee J, Wee S, Gunaratne J, Chua RJE, Smith RAA, Ling L, Fernig DG, Swaminathan K, Nurcombe V, Cool SM. Structural determinants of heparin-transforming growth factor- $\beta$ 1 interactions and their effects on signaling. *Glycobiology*. 2015; 25(12):1491–1504. [PubMed: 26306634]
24. McCaffrey TA, Falcone DJ, Vicente D, Du B, Consigli S, Borth W. Protection of transforming growth factor-beta 1 activity by heparin and fucoidan. *Journal of cellular physiology*. 1994; 159(1): 51–59. [PubMed: 7511146]
25. McCaffrey TA, Falcone DJ, Brayton CF, Agarwal LA, Welt FG, Weksler BB. Transforming growth factor-beta activity is potentiated by heparin via dissociation of the transforming growth factor-beta/alpha 2-macroglobulin inactive complex. *The Journal of cell biology*. 1989; 109(1):441–448. [PubMed: 2473082]

26. Bhaskar U, Hickey AM, Li G, Mundra RV, Zhang F, Fu L, Cai C, Ou Z, Dordick JS, Linhardt RJ. A purification process for heparin and precursor polysaccharides using the pH responsive behavior of chitosan. *Biotechnology progress*. 2015; 31(5):1348–1359. [PubMed: 26147064]
27. Bhatia SN, Balis UJ, Yarmush ML, Toner M. Effect of cell-cell interactions in preservation of cellular phenotype: cocultivation of hepatocytes and nonparenchymal cells. *The FASEB journal: official publication of the Federation of American Societies for Experimental Biology*. 1999; 13(14):1883–1900. [PubMed: 10544172]
28. Guillouzo A. Liver cell models in in vitro toxicology. *Environmental health perspectives*. 1998; 106(Suppl 2):511–532. [PubMed: 9599700]
29. Khetani SR, Szulgit G, Del Rio JA, Barlow C, Bhatia SN. Exploring interactions between rat hepatocytes and nonparenchymal cells using gene expression profiling. *Hepatology (Baltimore, Md)*. 2004; 40(3):545–554.
30. Khetani SR, Chen AA, Ranscht B, Bhatia SN. T-cadherin modulates hepatocyte functions in vitro. *The FASEB journal: official publication of the Federation of American Societies for Experimental Biology*. 2008; 22(11):3768–3775. [PubMed: 18635739]
31. Lin C, Shi J, Moore A, Khetani SR. Prediction of Drug Clearance and Drug-Drug Interactions in Microscale Cultures of Human Hepatocytes. *Drug metabolism and disposition: the biological fate of chemicals*. 2016; 44(1):127–136. [PubMed: 26452722]
32. Wang WW, Khetani SR, Krzyzewski S, Duignan DB, Obach RS. Assessment of a Micropatterned Hepatocyte Coculture System to Generate Major Human Excretory and Circulating Drug Metabolites. *Drug metabolism and disposition: the biological fate of chemicals*. 2010; 38(10):1900–1905. [PubMed: 20595376]
33. Ramsden D, Tweedie DJ, Chan TS, Taub ME, Li Y. Bridging in vitro and in vivo metabolism and transport of faldaprevir in human using a novel cocultured human hepatocyte system, HepatoPac. *Drug metabolism and disposition: the biological fate of chemicals*. 2014; 42(3):394–406. [PubMed: 24366904]
34. Khetani SR, Kanchagar C, Ukairo O, Krzyzewski S, Moore A, Shi J, Aoyama S, Aleo M, Will Y. Use of micropatterned cocultures to detect compounds that cause drug-induced liver injury in humans. *Toxicological sciences: an official journal of the Society of Toxicology*. 2013; 132(1):107–117. [PubMed: 23152190]
35. Ploss A, Khetani SR, Jones CT, Syder AJ, Trehan K, Gaysinskaya VA, Mu K, Ritola K, Rice CM, Bhatia SN. Persistent hepatitis C virus infection in microscale primary human hepatocyte cultures. *Proceedings of the National Academy of Sciences*. 2010; 107(7):3141–3145.
36. Shlomai A, Schwartz RE, Ramanan V, Bhatta A, de Jong YP, Bhatia SN, Rice CM. Modeling host interactions with hepatitis B virus using primary and induced pluripotent stem cell-derived hepatocellular systems. *Proceedings of the National Academy of Sciences*. 2014; 111(33):12193–12198.
37. March S, Ng S, Velmurugan S, Galstian A, Shan J, Logan DJ, Carpenter AE, Thomas D, Sim BKL, Mota MM, et al. A microscale human liver platform that supports the hepatic stages of *Plasmodium falciparum* and *vivax*. *Cell host & microbe*. 2013; 14(1):104–115. [PubMed: 23870318]
38. Davidson MD, Ballinger KR, Khetani SR. Long-term exposure to abnormal glucose levels alters drug metabolism pathways and insulin sensitivity in primary human hepatocytes. *Scientific reports*. 2016; 6:28178. [PubMed: 27312339]
39. Davidson MD, Lehrer M, Khetani SR. Hormone and Drug-Mediated Modulation of Glucose Metabolism in a Microscale Model of the Human Liver. *Tissue engineering. Part C, Methods*. 2015; 21(7):716–725.
40. Kidambi S, Yarmush RS, Novik E, Chao P, Yarmush ML, Nahmias Y. Oxygen-mediated enhancement of primary hepatocyte metabolism, functional polarization, gene expression, and drug clearance. *Proceedings of the National Academy of Sciences of the United States of America*. 2009; 106(37):15714–15719. [PubMed: 19720996]
41. Baghy K, Iozzo RV, Kovalszky I. Decorin-TGF $\beta$  axis in hepatic fibrosis and cirrhosis. *The journal of histochemistry and cytochemistry: official journal of the Histochemistry Society*. 2012; 60(4):262–268. [PubMed: 22260996]

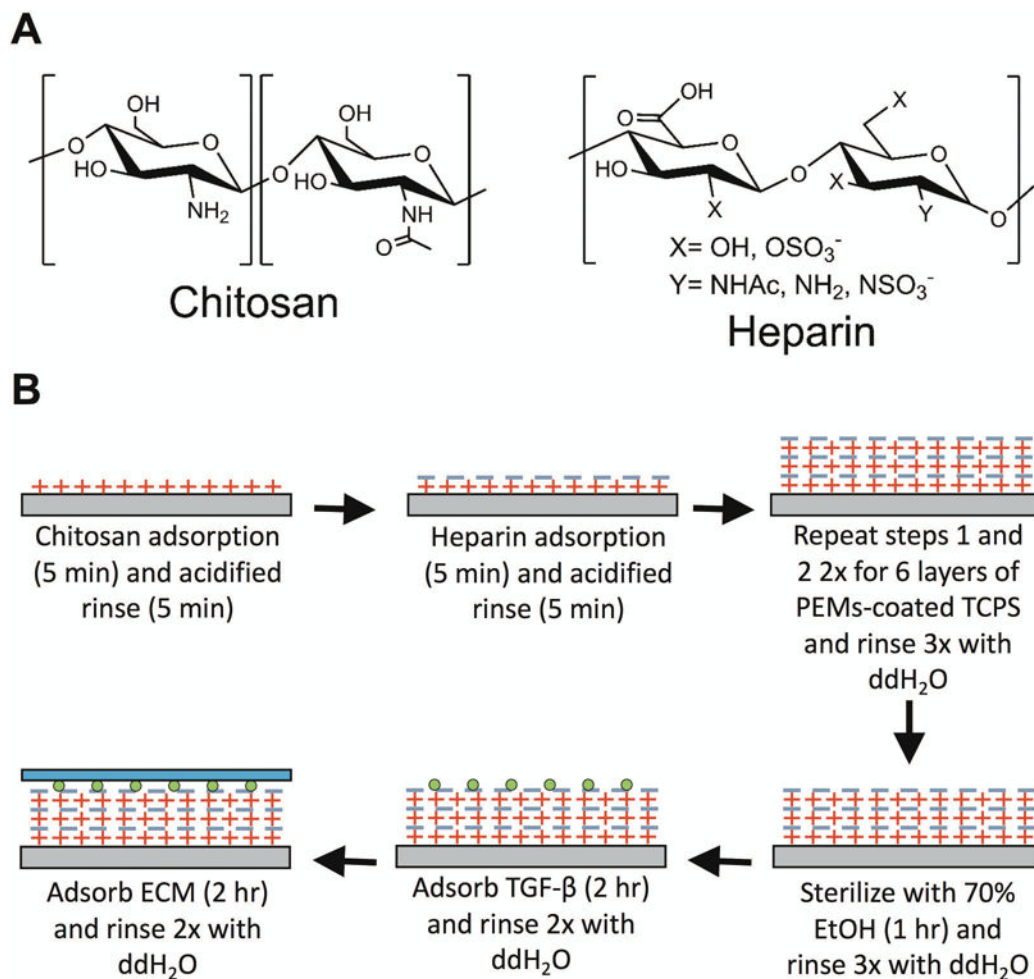


**Figure 1. Fabrication of polyelectrolyte multilayers (PEMs) containing layers of chitosan and heparin on tissue culture polystyrene (TCPS) for cell attachment and growth factor delivery** (A) Chemical structures of the chitosan (left) and heparin (right) used to assemble PEMs. (B) Process steps for first fabricating PEMs on TCPS (top row). The PEM-adsorbed TCPS plates are then sterilized using 70% vol/vol ethanol (EtOH) prior to modifying the PEMs with a growth factor such as transforming growth factor beta (TGFβ) and extracellular matrix (ECM) proteins such as collagen, fibronectin, or Matrigel (bottom row).



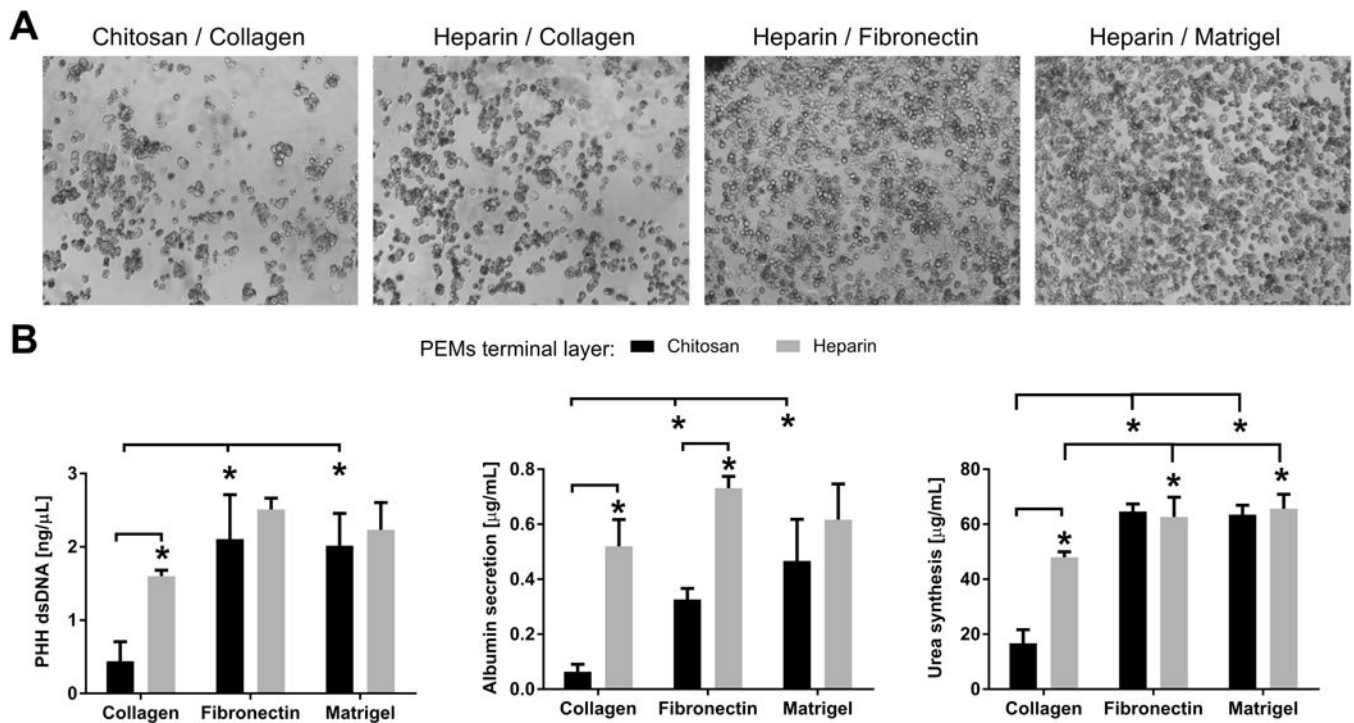


**Figure 2. Effects of polyelectrolyte terminal layer and extracellular matrix (ECM) protein on adhesion and functions of primary human hepatocytes (PHHs)**

(A) Phase contrast images (1 day after cell seeding) of PHHs adhered to polyelectrolyte multilayers (PEMs) of the indicated terminal layer (chitosan or heparin) and adsorbed ECM protein (rat tail type I collagen, fibronectin, and Matrigel at 100  $\mu\text{g}/\text{mL}$  density in solution).

(B) Left: Quantification of double-stranded DNA (dsDNA) from adherent PHHs (9 days after cell seeding) on either chitosan- or heparin-terminated PEMs modified with different ECM proteins. Middle: Cultures as in those created for dsDNA quantification except albumin secretion after 4 days is shown. Right: Same cultures as those used for albumin secretion analysis except urea levels were quantified from the same cell culture supernatants.

\* $P < 0.05$  (one-way ANOVA and Tukey's *post-hoc* test).

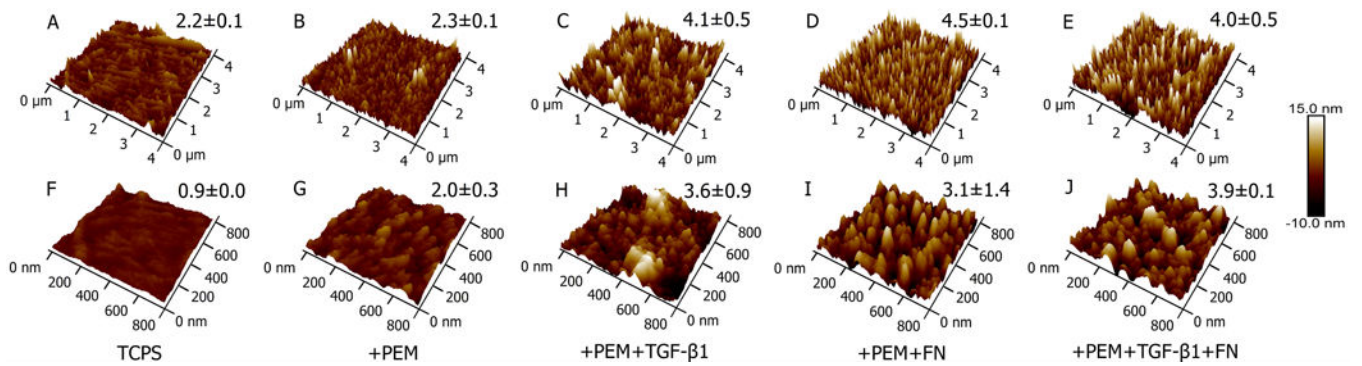


**Figure 3. Atomic force microscopy (AFM) micrographs of tissue culture polystyrene (TCPS) modified with heparin-terminated polyelectrolyte multilayers (PEMs), transforming growth factor beta (TGF $\beta$ ), and fibronectin (FN)**

(A–E, top row) 4  $\mu\text{m}$   $\times$  4  $\mu\text{m}$  and (F–J, bottom row) 800 nm  $\times$  800 nm scan size micrographs with subsequent TCPS modification steps. Subsequent surface modifications show increased surface features and increased average root mean square roughness (Rq). Average Rq and standard deviation are shown.

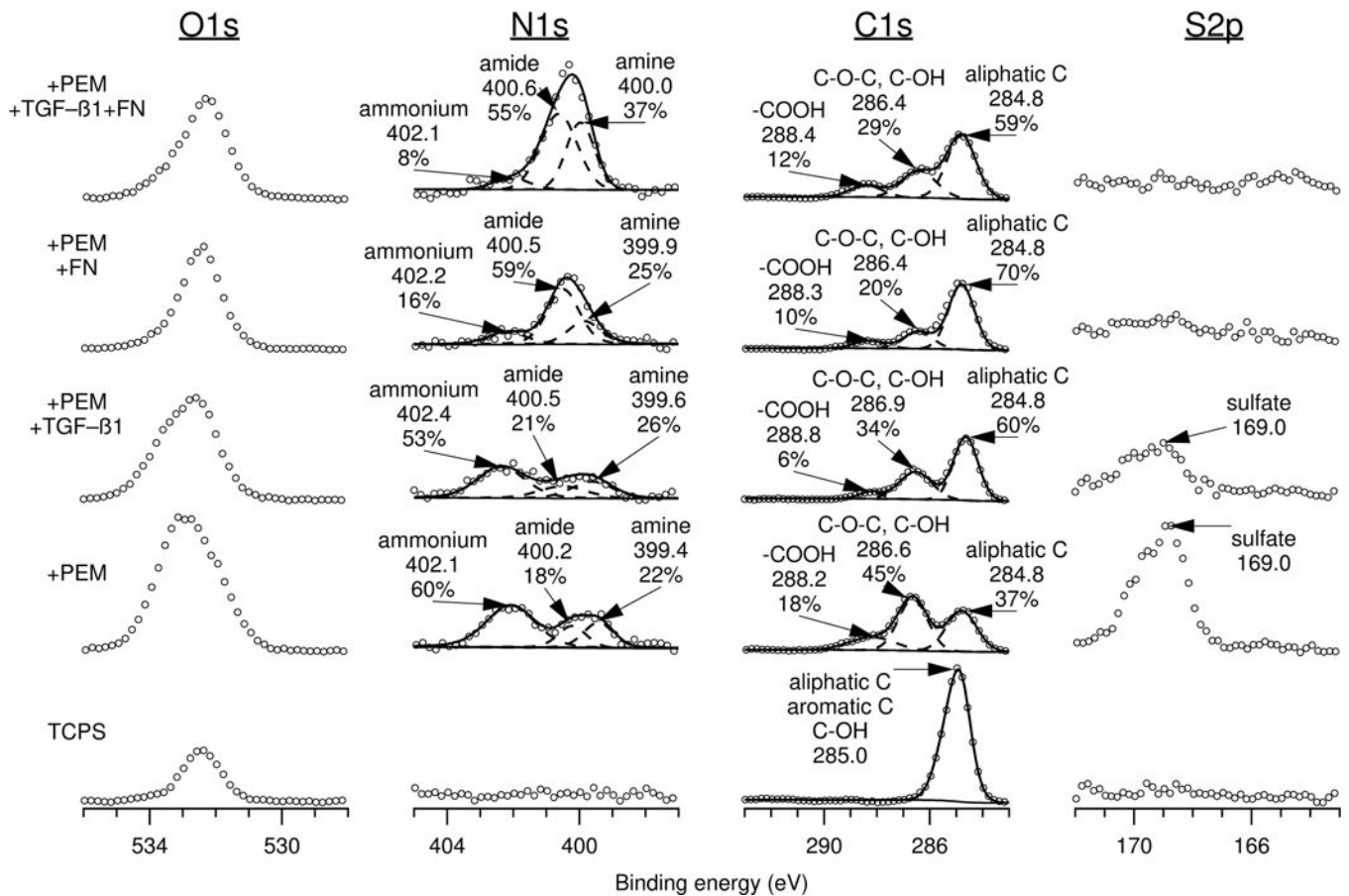


**Figure 4. X-ray photoelectron spectroscopy (XPS) high resolution spectra of O1s, N1s, C1s, and S2p envelopes of tissue culture polystyrene (TCPS) modified with heparin-terminated polyelectrolyte multilayers (PEMs), transforming growth factor beta (TGFβ), and fibronectin (FN)**

Attenuation of the sulfate peak (169.0 eV) and changes in the N1s envelope in protein-coated PEMs compared to protein-free PEMs supports protein adsorption onto heparin-terminated PEMs on TCPS.

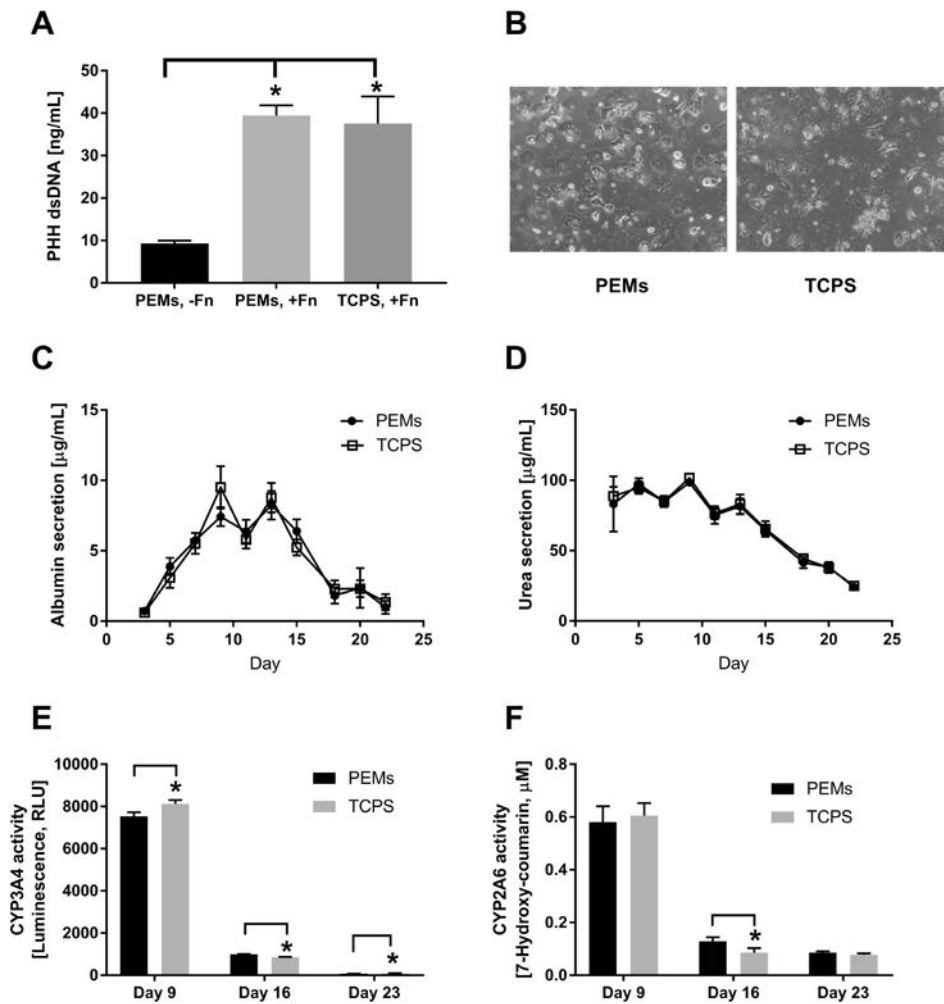


**Figure 5. Comparison of primary human hepatocyte (PHH) functions on polyelectrolyte multilayers (PEMs) and tissue culture polystyrene (TCPS) substrates**  
**(A)** Quantification of double-stranded DNA (dsDNA) from adherent PHHs (1 day after cell seeding) on heparin-terminated PEMs without fibronectin (-Fn), heparin-terminated PEMs modified with 100 µg/mL of fibronectin (+Fn) or TCPS with 100 µg/mL of fibronectin. **(B)** Phase contrast images (from day 5 of culture) of PHHs adhered to heparin-terminated PEMs or TCPS modified with 100 µg/mL of fibronectin. **(C)** Albumin secretion over 3 weeks on heparin-terminated PEMs or TCPS, both modified with 100 µg/mL of fibronectin. **(D)** Urea secretion over time from the same cultures as those used in panel C. **(E)** Cytochrome P450 3A4 (CYP3A4) enzyme activity in the same cultures as those used in panel C. **(F)** CYP2A6 enzyme activity in the same cultures as those used in panel C. \* $P < 0.05$  (one-way ANOVA and Tukey's *post-hoc* test for panel A and Student's two-tailed t-test for panels E and F).

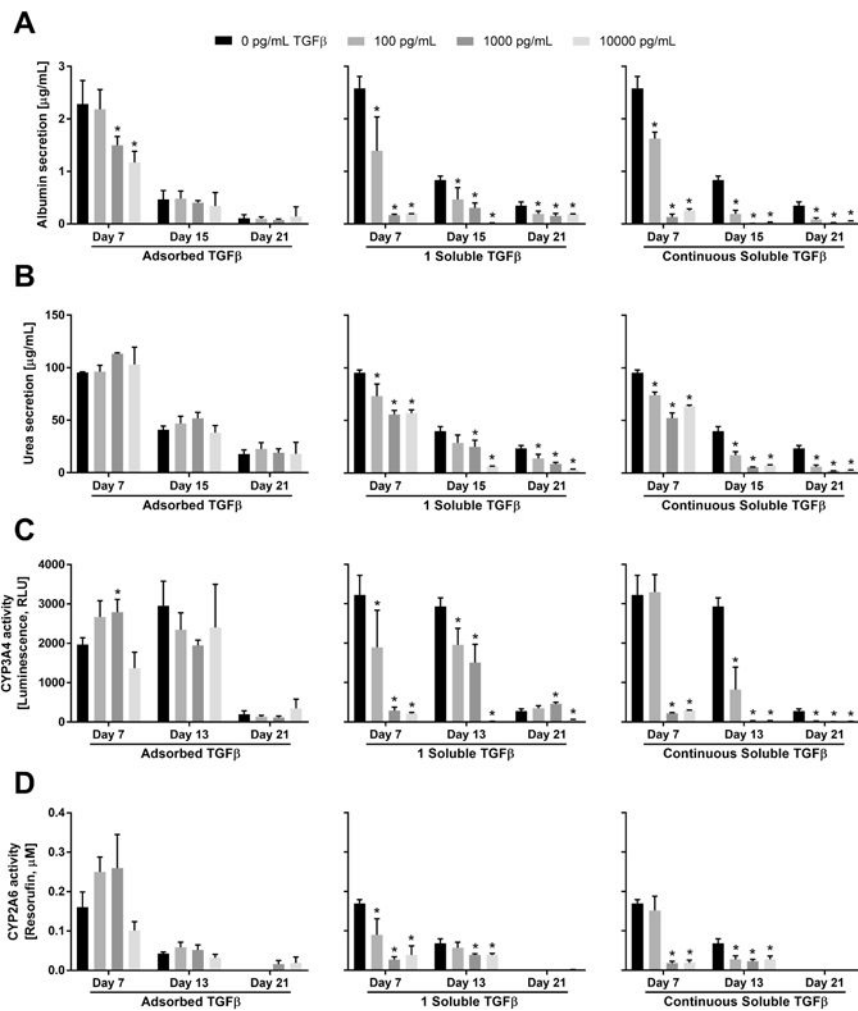


**Figure 6. Modulation of primary human hepatocyte (PHH) functions by the presentation of transforming growth factor beta (TGF $\beta$ ) either adsorbed to heparin-terminated polyelectrolyte multilayers (PEMs) or in solution once (1 soluble) or continuously with culture medium changes** For the adsorbed TGF $\beta$  conditions, PEMs were created as shown in figure 1B using 100  $\mu\text{g/mL}$  of fibronectin for cell attachment and varying concentrations of TGF $\beta$ . For the soluble TGF $\beta$  conditions, PHH cultures were established on standard tissue culture polystyrene (TCPS) plates modified with 100  $\mu\text{g/mL}$  of fibronectin. **(A)** Albumin secretion over 3 weeks from PHH cultures at the indicated concentrations of either adsorbed TGF $\beta$  (left), soluble TGF $\beta$  delivered once over a 2-day media exchange (middle), or soluble TGF $\beta$  delivered with every 2-day medium exchanges (right). **(B)** Urea secretion from the same cultures as those used for panel A. **(C)** Cytochrome P450 3A4 (CYP3A4) enzyme activity in the same cultures as those used for panel A. **(D)** CYP2A6 enzyme activity in the same cultures as those used for panel A. Asterisks indicate statistically significant differences between the condition and the TGF $\beta$ -free control for that specific timepoint with  $P < 0.05$  (one-way ANOVA and Dunnett's *post-hoc* test).

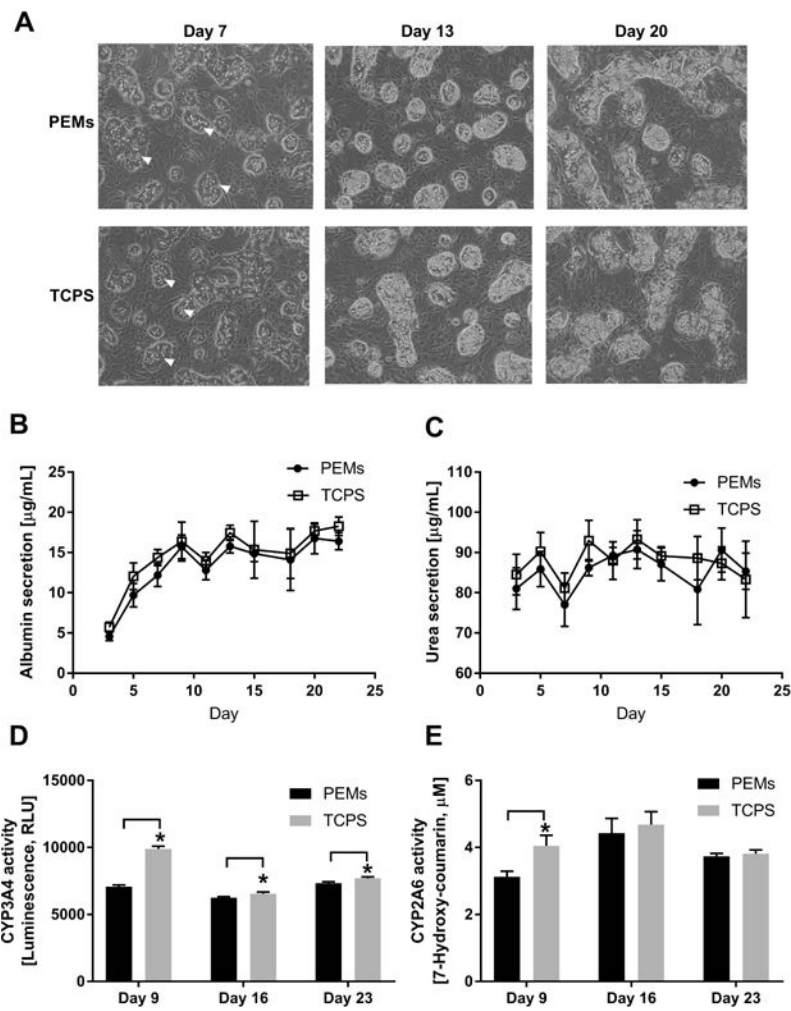


**Figure 7. Creation of co-cultures of primary human hepatocytes (PHHs) and 3T3-J2 murine embryonic fibroblasts on polyelectrolyte multilayers (PEMs) and assessment of long-term morphology and liver functions**

(A) Phase contrast images of co-cultures on heparin-terminated PEMs or TCPS modified with fibronectin for cell attachment. White arrowheads indicate PHHs. (B) Albumin secretion from co-cultures created as in panel A. (C) Urea secretion over time in the same cultures as those used for panel A. (D) Cytochrome P450 3A4 (CYP3A4) enzyme activity in the same cultures as those used for panel A. (E) CYP2A6 enzyme activity in the same cultures as those used for panel A. \* $P < 0.05$  (Student's two-tailed t-test).

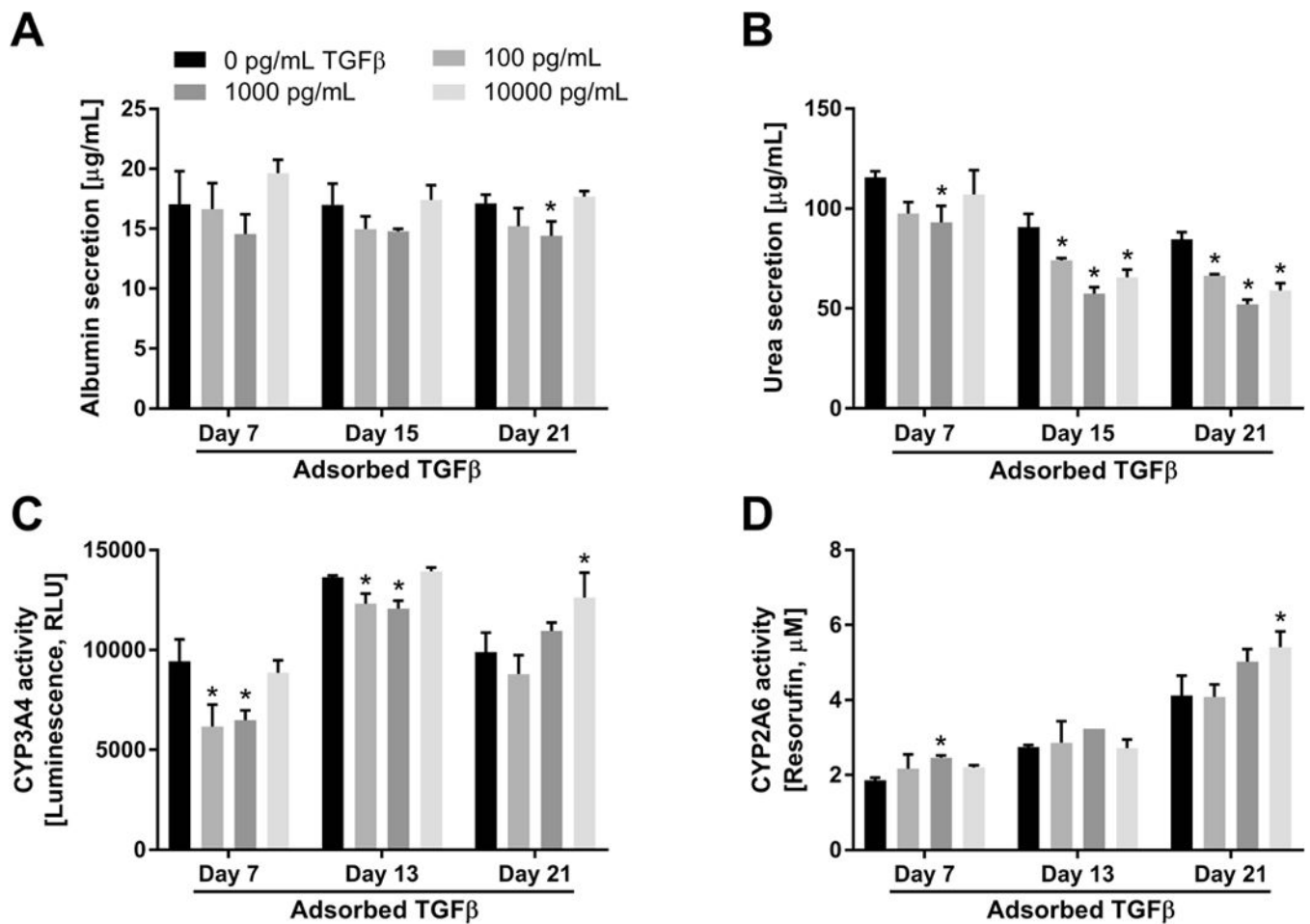


**Figure 8. Modulation of functions in co-cultures of primary human hepatocytes (PHHs) and 3T3-J2 murine embryonic fibroblasts by the presentation of transforming growth factor beta (TGFβ) adsorbed to heparin-terminated polyelectrolyte multilayers (PEMs)**

PEMs were created as shown in figure 1B using of 100  $\mu\text{g/mL}$  fibronectin for cell attachment and varying concentrations of adsorbed TGFβ. (A) Albumin secretion from co-cultures on PEMs modified with fibronectin and the indicated concentrations of adsorbed TGFβ. (B) Urea secretion from the same cultures as those used for panel A. (C) Cytochrome P450 3A4 (CYP3A4) enzyme activity in the same cultures as those used for panel A. (D) CYP2A6 enzyme activity in the same cultures as those used for panel A. Asterisks indicate statistically significant differences between the condition and the TGFβ-free control for that specific timepoint with  $P < 0.05$  (one-way ANOVA and Dunnett's *post-hoc* test).

**Table 1**  
**X-ray photoelectron spectroscopy (XPS) Average Atomic Percentages**

Polyelectrolyte multilayers (PEMs) of chitosan and heparin (terminal layer) were created on tissue culture polystyrene (TCPS). Then, transforming growth factor  $\beta$  (TGF $\beta$ ) or fibronectin (FN, 100  $\mu\text{g}/\text{mL}$ ) or both were adsorbed on the PEMs as shown in Figure 1. XPS was performed on the samples as described in the Methods section. 'N.D.' indicates that value could not be measured.

Treatment Group	O1s	N1s	C1s	S2p	C/O	N/S
TCPS	13.0 $\pm$ 1.3	N.D.	76.8 $\pm$ 2.2	N.D.	5.9 $\pm$ 0.8	N.D.
+PEM	34.6 $\pm$ 0.9	4.5 $\pm$ 0.4	54.7 $\pm$ 0.5	2.9 $\pm$ 0.3	1.6 $\pm$ 0.1	1.6 $\pm$ 0.0
+PEM+TGF $\beta$	28.8 $\pm$ 1.2	3.7 $\pm$ 1.5	55.4 $\pm$ 2.6	1.5 $\pm$ 0.4	1.9 $\pm$ 0.0	2.4 $\pm$ 0.4
+PEM+FN	25.1 $\pm$ 1.9	6.3 $\pm$ 3.5	56.9 $\pm$ 2.7	0.7 $\pm$ 0.3	2.3 $\pm$ 0.3	10.4 $\pm$ 8.8
+PEM+TGF $\beta$ +FN	24.5 $\pm$ 0.0	6.2 $\pm$ 1.4	56.5 $\pm$ 2.2	1.2 $\pm$ 0.4	2.3 $\pm$ 0.1	5.8 $\pm$ 3.1



**Table 2**  
**Average TGFβ percent cumulative release and retention over 3 days**

Polyelectrolyte multilayers (PEMs) of chitosan and heparin (terminal layer) were created on tissue culture polystyrene (TCPS). Then, transforming growth factor β (TGFβ) or fibronectin (FN, 100 μg/mL) or both were adsorbed on the PEMs as shown in Figure 1. TGFβ was quantified in the supernatant to determine potential release following adsorption to the heparin-terminated PEMs. Estimates are given when ELISA response of samples was below the lower limit of detection. 'N.D.' indicates that TGFβ concentration could not be determined in the supernatant, suggesting that the majority of the TGFβ was still retained on the heparin-terminated PEMs.

TGFβ (pg/ml)	FN	Average TGFβ mass bound to PEMs (pg)	% Cumulative TGFβ release			% Cumulative TGFβ retention		
			D0 (2 h)	D1	D3	D0 (2 h)	D1	D3
10,000	-	545.2	9.8	11.4	11.4 - 13.2	90.2	88.6	86.8 - 88.6
1000	-	42.7	15.1	15.1 - 22.6	N.D.	84.9	77.4 - 84.9	N.D.
100	-	1.8 - 5.2	N.D.	N.D.	N.D.	N.D.	N.D.	N.D.
10,000	+	542.3	13.4	15.7	15.7 - 17.5	86.6	84.3	82.5 - 84.3
1000	+	42.9	21.5	29.5	29.5 - 52.6	78.5	70.5	47.4 - 70.5
100	+	1.8 - 5.2	N.D.	N.D.	N.D.	N.D.	N.D.	N.D.